TU Delft

Delft University of Technology

Examining Contrail Formation Models with Open Flight and Remote Sensing Data

Roosenbrand, E.J.; Sun, Junzi; Hoekstra, J.M.

Publication date
2022

Document Version
Final published version

Citation (APA)
Roosenbrand, E. J., Sun, J., & Hoekstra, J. M. (2022). *Examining Contrail Formation Models with Open Flight and Remote Sensing Data*. 1-8. Paper presented at 12th SESAR Innovation Days, Budapest, Hungary.

Important note
To cite this publication, please use the final published version (if applicable).
Please check the document version above.

Copyright
Other than for strictly personal use, it is not permitted to download, forward or distribute the text or part of it, without the consent of the author(s) and/or copyright holder(s), unless the work is under an open content license such as Creative Commons.

Takedown policy
Please contact us and provide details if you believe this document breaches copyrights.
We will remove access to the work immediately and investigate your claim.

This work is downloaded from Delft University of Technology.
For technical reasons the number of authors shown on this cover page is limited to a maximum of 10.

Green Open Access added to TU Delft Institutional Repository

'You share, we take care!' - Taverne project

https://www.openaccess.nl/en/you-share-we-take-care

Otherwise as indicated in the copyright section: the publisher is the copyright holder of this work and the author uses the Dutch legislation to make this work public.

Examining Contrail Formation Models with Open Flight and Remote Sensing Data

Esther Roosenbrand, Junzi Sun and Jacco Hoekstra
Control and Simulation, Faculty of Aerospace Engineering
Delft University of Technology, The Netherlands

***Abstract*—One of the biggest challenges facing the aerospace industry today is its sustainability. As the number of flights is expected to rise globally, aviation's climate impact will continue to increase. Current research has extensively addressed the rerouting of aircraft through wind-optimization in order to minimize fuel burn and emissions. Such optimization is currently implemented for flight planning. Although this strategy is optimized for fuel burn and emissions, it does not necessarily minimize the overall climate impact. Navigating optimally through wind fields could mean flying through regions with a higher climate impact, where warming contrails are formed. This can occur when contrails trap outgoing terrestrial radiation and so contribute to global warming. This warming contrail creation could potentially forfeit the climate gain of the reduced emissions from the wind-optimized route. In order to implement such a climate-optimized routing model, knowledge about the atmospheric conditions under which contrails form is required. One existing theorem is the Schmidt-Appleman Criterion, which uses the air temperature, relative humidity and ambient air pressure to determine whether contrail formation is possible. In addition, the ice-supersaturation criterion model indicates contrail persistence. In this paper, multiple open data sources are used to examine the use of this established criterion, to evaluate the appropriateness of these data sources for future use in a climate-optimized routing model. Based on the obtained results, we show that, with these data sources, the combination of Schmidt-Appleman and the ice-supersaturation criterion can produce a more reliable determination of contrail formation. The results can be used for an improved unified and data-driven model for the purposes of climate-optimized routing.**

***Keywords*—Sustainability, Contrails, Remote Sensing, Atmospheric Science, OpenSky, Aircraft Surveillance Data**

I. Introduction

Currently global aviation contributes to approximately 5% of net anthropogenic climate forcing [1]. During the energy transition, other sectors will likely reduce their climate impact at a faster pace than aviation, causing the relative contribution of aviation to rise over the coming years. Over recent years, societal pressure has also been growing for a more sustainable aerospace industry. Besides the fact that effective sustainability measures (such as alternative fuels and aerodynamic aircraft design) are still under development, their implementation on a commercially relevant scale is expected to take years, and perhaps even decades. In order to meet the urgency of the climate crisis, the focus of sustainable aviation should also be on what is safely implementable and possible today or within the next few years with the operations of today's aircraft. The application of multidisciplinary fields beyond aviation alone, such as combining global aircraft surveillance data, atmospheric science, and satellite remote sensing, can help solve this challenge in the form of a climate optimized trajectory model.

The climate optimized trajectory model proposed in our earlier research [2] deviates from a standard wind-optimized route in that it will take into account contrail forming areas, thus minimizing the additional contrail energy forcing. Energy forcing (EF) provides a unit for the contrail climate forcing for an individual flight, integrating the contrails radiative forcing (RF), width, length and lifetime [3]. While CO_2 accounts for a third of global effective radiative forcing (ERF) from aviation, non-CO_2 (mainly from contrail formation and NO_x) accounts for the other two-thirds [1], [4]. ERF differs from EF, as it accounts for second-order atmospheric responses caused by contrails [3]. It has been suggested that the global mean ERF of contrails is larger than the ERF of aviation's cumulative CO_2 emissions since the start of commercial air travel [1], [5]. To minimize additional energy forcing, it is advantageous to create contrails in some situations whereas it is disadvantageous in others. The energy forcing from emissions produced by the detour from the wind-optimized trajectory must be offset against the forcing gained or lost by contrails formed to assure a fully climate-optimized route. This approach requires knowledge about the atmospheric conditions under which contrails form. As a general rule, contrails form under high humidity and low temperature conditions [6]. Hot water vapor emissions and soot from aircraft exhaust mix with the cooler ambient air, which causes an increase in the local relative humidity [3]. When this exceeds the liquid saturation level, liquid water droplets form on the surface of the soot particles, after which they freeze into ice crystals, causing contrails to form.

These atmospheric conditions are captured by the Schmidt-Appleman criterion (SAC), which predicts the propensity of contrail formation [6]. The persistence of a contrail, an important parameter for its climate impact is indicated by the presence of an ice-supersaturation region (ISSR). An essential quality of the climate optimized model is its ability to predict contrail formation based on open flight and remote sensing data, and verification that the data selected is suitable to predict contrail formation is necessary. This paper endeavours to examine whether the open source datasets (described in section III), in combination with the SAC (section II-C) and ISSR criterion (section II-B) can adequately predict contrail formation. The results are shown in section IV.

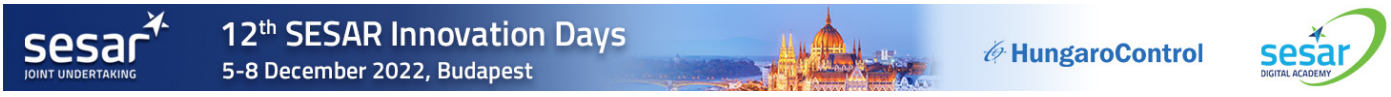

II. Method

A. The Schmidt-Appleman Criterion

Contrails, cloud-like in appearance, can be formed in the wake of aircraft. For contrail formation to occur, the temperature of the air should be below -40°C (233.15 K), with a high relative humidity [7]. The Schmidt-Appleman Criterion (SAC) is a thermodynamic theory deduced by Schmidt and Appleman and re-examined by Schumann [7], showing that the threshold condition for contrail formation from condensing exhaust water depends on ambient pressure, humidity and the ratio of water and heat released into the exhaust plume. When an aircraft flies through atmospheric conditions that satisfy SAC, saturation with respect to liquid water occurs, and a contrail is formed. This threshold temperature for contrail formation depends on the ambient relative humidity and on the slope of the isobaric mixing line (G), which is given by:

$$G = \frac{EI_{H_2O}\ c_p\ p}{\varepsilon\ Q\ (1-\eta)} \tag{1}$$

where constants are defined in Table I.

TABLE I. Constants used in Schmidt-Appleman Criterion

Symbol	Constant	Value	Unit
EI_{H_2O}	Emission index	1.2232	$-\ (kg_{H_2O}\ kg_{fuel}^{-1})$
c_p	Specific heat capacity air	1004	$J\ kg^{-1}\ K^{-1}$
ε	Ratio molar mass of water vapor and air	0.622	-
Q	Specific combustion heat	43×10^6	$J\ kg^{-1}$

The isobaric missing line, G, is also dependent on the ambient pressure p_h at the flight level and the overall propulsion efficiency (η) is given by the ratio:

$$\eta = \frac{FV}{m_f Q} \tag{2}$$

where FV indicates the work rate (thrust F of engine at true air speed V), and $m_f Q$ is the amount of chemical energy provided by fuel with specific combustion heat Q at a flow rate of m_f. Similar to as seen in literature [8], an overall propulsion efficiency (η) of 0.4 is assumed.

The threshold temperature (T_{LC}) is the temperature at which the saturation vapor pressure with respect to ice and the mixing line intersect. The saturation vapor pressure over water curve is plotted in blue in Fig. 1 and is given by the Goff-Gratch equation [9]:

$$\begin{aligned}\log\ e^*_{water} = &-7.90298 \cdot (\frac{T_{st}}{T} - 1) + 5.02808 \cdot \log(\frac{T_{st}}{T}) \\ &- 1.3816 \times 10^{-7} \cdot (10^{11.344 \cdot (1 - T/T_{st})} - 1) \\ &+ 8.1328 \times 10^{-3} \cdot (10^{-3.49149 \cdot (T_{st}/T - 1)} - 1)\end{aligned}$$

with T as the temperature and T_{st} as the steam point temperature (372.15 K).

The saturation vapor pressure over ice is plotted in orange in Fig. 1 and is given by:

$$\begin{aligned}\log\ e^*_{ice} = &-9.09718 \cdot (T_0/T - 1) + 3.56654 \cdot \log(T_0/T) \\ &+ 0.876793 \cdot (1 - T/T_0)\end{aligned}$$

where T_0 is the ice-point temperature (273.16 K).

Before the threshold value T_{LC} can be determined, the temperature T_{LM} has to be identified first, given by:

$$T_{LM} = -46.46 + 9.43 \ln(G - 0.053) + 0.720[\ln(G - 0.053)]^2$$

Subsequently, the mixing line is defined as the tangent line at the T_{LM} point with the saturation water vapor pressure curve (given by e^*). The T_{LC} is the intersection of the mixing line and the saturation water vapor pressure curve over ice. This geometric approach to identifying the T_{LC}, is visualized in Fig. 1.

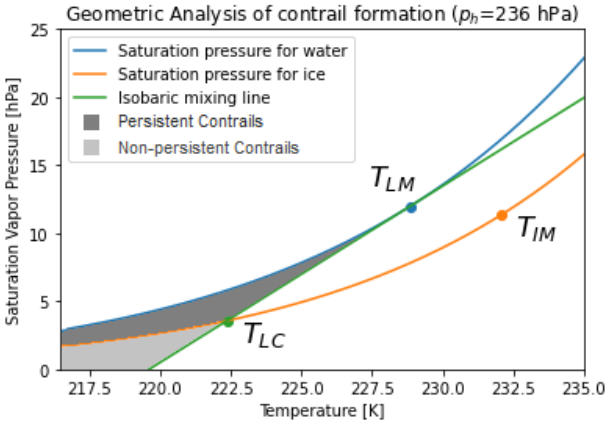

Figure 1. A visualization of the geometric approach to determining the critical formation temperature (T_{LC}), using the saturation pressure for water, the saturation pressure for ice and the isobaric mixing line with slope G at p_h = 230 hPa. Zones of contrails persistence are also indicated in the graph.

While Fig. 1 shows the formation temperature at a single altitude, Fig. 2 shows this T_{LC} plotted for a range of altitudes and relative humidities in a single plot.

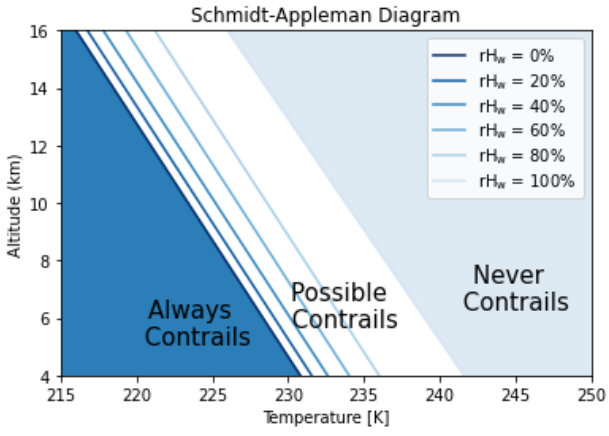

Figure 2. A Schmidt-Appleman Diagram where the solid lines indicate the threshold temperatures at 0, 20, 40, 60, 80 and 100% relative humidity respectively, for kerosene fuel and an overall propulsion efficiency of 0.4.

sesar JOINT UNDERTAKING 12th SESAR Innovation Days 5-8 December 2022, Budapest HungaroControl sesar DIGITAL ACADEMY

Fig. 2 can be subdivided in three sections; always contrails, possible contrails and never contrails. In the case where the ambient temperature falls above the line of relative humidity with respect to water (rH_w) of 100%, contrails should never form [10], [11]. In conditions where the ambient temperature falls below the relative humidity line of 0%, contrails should always form. When the point is between these two lines, in the 'possible contrail' section of the graph, formation of contrails depends on the relative humidity at the point, whether it falls to the left (always contrail) or right (never contrail) side of the corresponding rH_w line.

B. Ice-supersaturation Condition

Some contrails disappear quickly, but persistent contrails, with lifetimes of more than a few minutes, occur when they do not evaporate when mixed with the environment [12]. Non-persistent contrails have a small to negligible climate impact [13]. Persistent contrails, which are relevant for our climate-optimal routing model, form when the ambient air is supersaturated with respect to ice [7], in ice-supersaturated regions (ISSR).

Those conditions can be found in Fig. 1, at temperatures lower than T_{LM} (temperature at which the mixing line is the tangent of the liquid saturation curve) in-between the curve of saturation pressure for water and the curve for ice [14]. Non-persistent contrails form at temperatures lower than T_{LC} under the saturation pressure for ice curve.

C. Persistent Contrail Formation

In summary, our climate-optimized routing model should be able to detect conditions that form persistent contrails, so flights which:

1) satisfies SAC, either by being in the 'Always Contrails' formation or in the 'Possible Contrail' (with the correct relative humidity) formation sections, indicating they can theoretically form *and*
2) fly through an ISSR, indicating they are persistent (and thus relevant for our model).

In the flowchart in Fig. 3, these conditions are visualized.

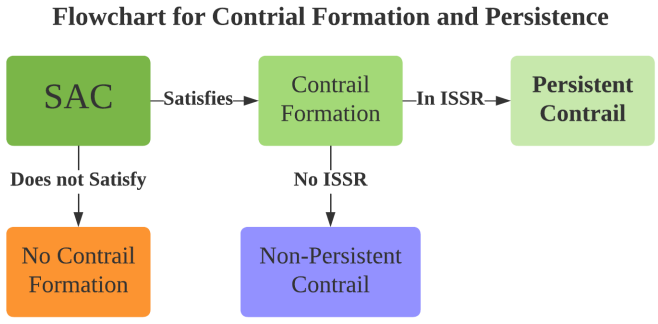

Figure 3. Flowchart regarding contrail formation and persistence. The relevant contrails for our climate-optimized routing model are the formations of persistent contrails, which must satisfy both SAC and ISSR presence.

III. Remote Sensing & Flight Data

For the examination of the contrail formation models, we categorize flights observations into binary 'contrail' (i.e. contrail observed) or 'no contrail' (i.e. no contrail observed) events. By comparing these two binary categories with the contrail formation models, predictions can be made based on atmospheric conditions, informing whether contrails can form. In this work, manual contrail identification based on the remote sensing and flight data is used. This section explains the data sources and the process used for the identification.

A. Remote Sensing data: GOES-16

Because contrails and cirrus clouds are atmospherically similar, infrared channels which are also used to identify cirrus clouds can be used to detect contrails, namely GOES-16 (channels 10.35 and 12.3 µm), with coverage over the USA. To eliminate background and ground information, a difference between channels is used in order to identify optically thin cirrus clouds. In these so-called brightness temperature differences (BTD) images, channels are subtracted from each other (12.3-10.35 µm) [15]. Fig. 4 shows an example of a BTD with contrails.

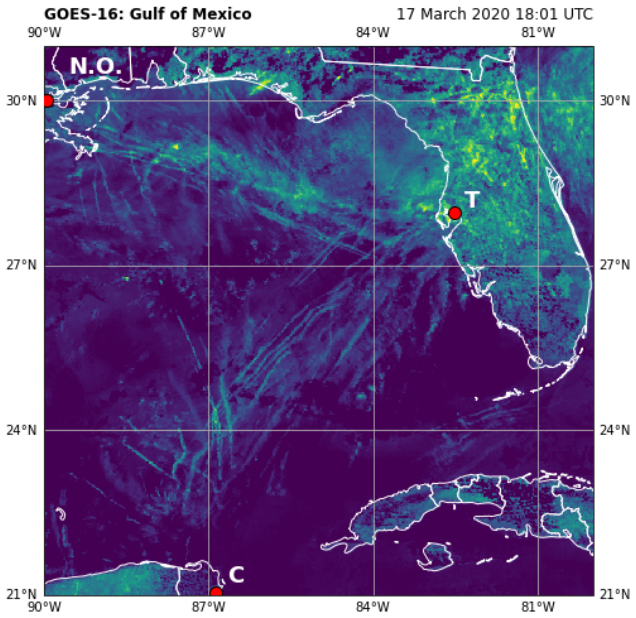

Figure 4. GOES-16 12.3-10.35 µm (BTD) image over the Gulf of Mexico, where contrails are visible of flights flying between i.a. New Orleans (N.O.), Tampa (T) and Cancún (C).

Since GOES is geostationary, it records every 5 min. This provides a temporal resolution high enough to allow for the observation of contrail formation. Using these BTD images and OpenSky ADS-B data, contrails can be detected and linked to the individual aircraft that formed them. By linking an individual aircraft with its own contrail, more information can be obtained about the type of contrail forming conditions, such as, temperature, atmospheric pressure, humidity, ice super-saturation (data from EUMETSAT), and aircraft altitude (OpenSky).

sesar JOINT UNDERTAKING 12th SESAR Innovation Days 5-8 December 2022, Budapest HungaroControl sesar DIGITAL ACADEMY

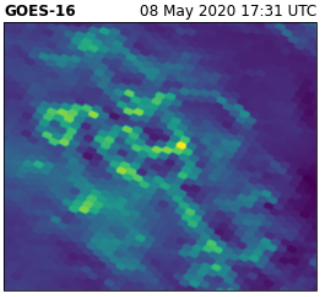

(a) GOES-16 BTD-image

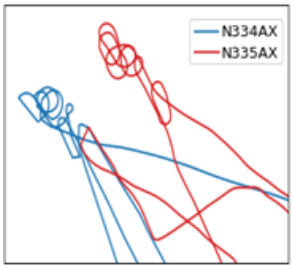

(b) OpenSky trajectories of N334AX and N335AX

(c) Terra MODIS: Corrected Reflectance (true color)

Figure 5. Contrails formed by military aircraft exercise on May 8th 2020, near Monterey Bay, California, USA, the time each of the measurements differs, which accounts for the slight differences in the images. (a) shows the GOES-16 BTD image, with winds blowing from the southeast and manipulating the contrail shape. (b) shows the full trajectory of the two military flights, and (c) shows a true color (RBG) image from MODIS.

This paper solely relies on GOES-16 data because of its high temporal resolution. Further, we focused in two areas known for contrail formation, the Gulf of California near San Francisco, and the Gulf of Mexico near western Florida's coast, since along the coast there is presence of humid cold air [16]. During the COVID-19 pandemic, the number of flights plummeted worldwide [17]. Because of the relatively open skies, attribution of single contrails to single aircraft is more straightforward, which is why dates in this time frame were selected. For this first test, seven days were identified, within the geographical and temporal boundaries described above, where contrails could be recognized individually.

B. Open flight data: OpenSky

The OpenSky Network has been collecting global air traffic surveillance data since 2013. The unfiltered and raw data is based on ADS-B, Mode S, TCAS and FLARM messages is open to use [18]. The variables used in this research include; time, latitude, longitude, callsign and the geoaltitude. Because of the high temporal and spacial resolution of OpenSky, the data can be integrated with GOES-16 imagery.

Flights were filtered to include only cruising or flights with small flight level changes (less than 1000 ft). In total, 235 flights were analysed. When multiple flights follow the same trajectory, it is unclear which specific aircraft in the sequence of flights creates a contrail. These flights are excluded from the analysis. In Fig. 5 three images are shown side by side of contrails formed by a military aircraft exercise. This figure demonstrates the two data sets described above and a true color (RGB) satellite image.

C. Atmospheric data: ECMWF

The parameters necessary to validate the Schmidt-Appleman criterion are air temperature, air pressure and relative humidity. At temperatures lower than -23°C (250.15K), the relative humidity data is calculated for saturation over ice instead of water by ECMWF. The aircraft geoaltitude from OpenSky is used to determine the pressure level. Based on the above methodology, it is determined whether the SAC can by applied to explain contrail formation in the labelled contrails.

Ice supersaturated regions (ISSR) can be very shallow in height (a few hundreds of meters), and so contrail formation is highly sensitive to altitude [16]. This requires the atmospheric data set to have a high vertical resolution, besides a high temporal resolution. Since generally, ISSR are laterally quite large [16], the spatial resolution of the data is less relevant.

The data was downloaded from the European Centre for Medium-Range Weather Forecasts (ECMWF) [19]. The spatial resolution of the ECMWF ERA-5 Reanalysis data is 0.25°× 0.25°and the temporal resolution is hourly. The vertical coverage has 37 pressure levels that range from 1000 hPa to 1 hPa. The relevant pressure levels for the proposes of this research range from 125 to 500 hPa, since these are the altitudes at which aircraft generally fly (11 to 16 km). Temperature and relative humidity are subsequently calculated based on the flight level.

IV. Analysis & Results

In this section, we focus on examining the Schmidt-Appleman Criterion, ice supersaturated regions, and our observation of contrails based on the flight and remote sensing data.

The sets of figures shown in this section are similar to the Schmidt-Appleman diagram in Fig. 2, in addition to points indicating an individual aircraft's altitude (from OpenSky) and ambient temperatures they are flying through (from ECMWF data). They were either observed to create contrails (marked in crosses) or not create contrails (colored circles). These colored circles are shaded to indicate the local relative humidity near the aircraft, with the same colormap as the rH_w lines. If a flight that was observed not to create contrails is flying through an ISSR, this is indicated by a red circle around the rH_w color indicator.

As described in the methodology section, for the purposes of our climate-optimized routing model it is important to predict persistent contrail formation, which is shown in Fig. 6 for both Florida (a), over three days and California (b), over four days. Non-persistent or no contrail formation should result in no rerouting from the model, and these are shown in Fig. 7. Since only flights at cruise are examined over the same geographical extent, there is an overlap of points present. The days vary in the amount of contrails formed, some days there is no contrail formation, other days an abundance of contrails are formed or in between.

sesar JOINT UNDERTAKING 12th SESAR Innovation Days 5-8 December 2022, Budapest HungaroControl sesar DIGITAL ACADEMY

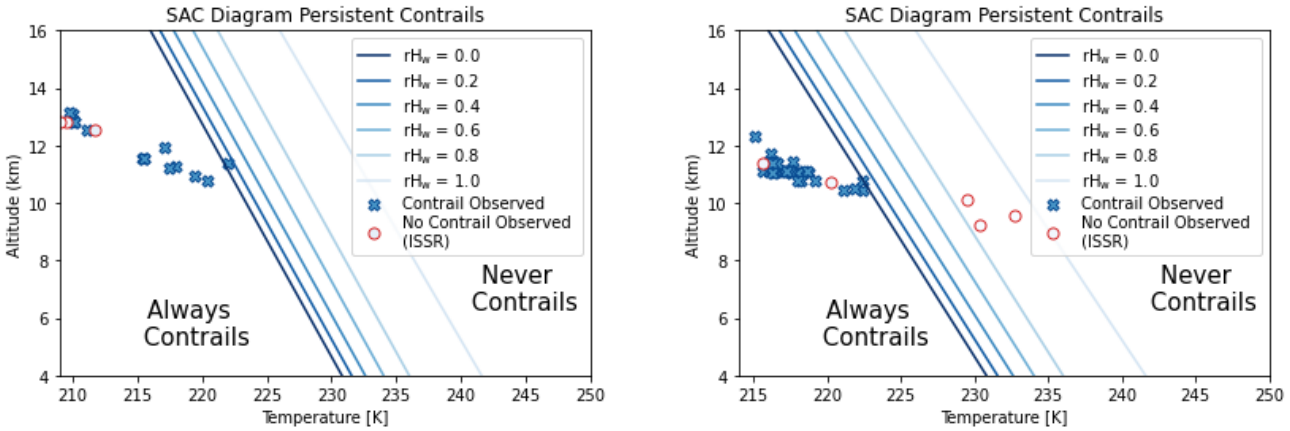

(a) SAC diagram for Persistent Contrails, Florida (16, 17 and 18 March 2020)

(b) SAC diagram for Persistent Contrails, California (6, 8, 9 and 10 May 2020)

Figure 6. **Persistent contrails** over Florida (a) and California (b). They must satisfy both the Schmidt-Appleman criteria (SAC) **and** occur in ice super saturated regions (ISSR)

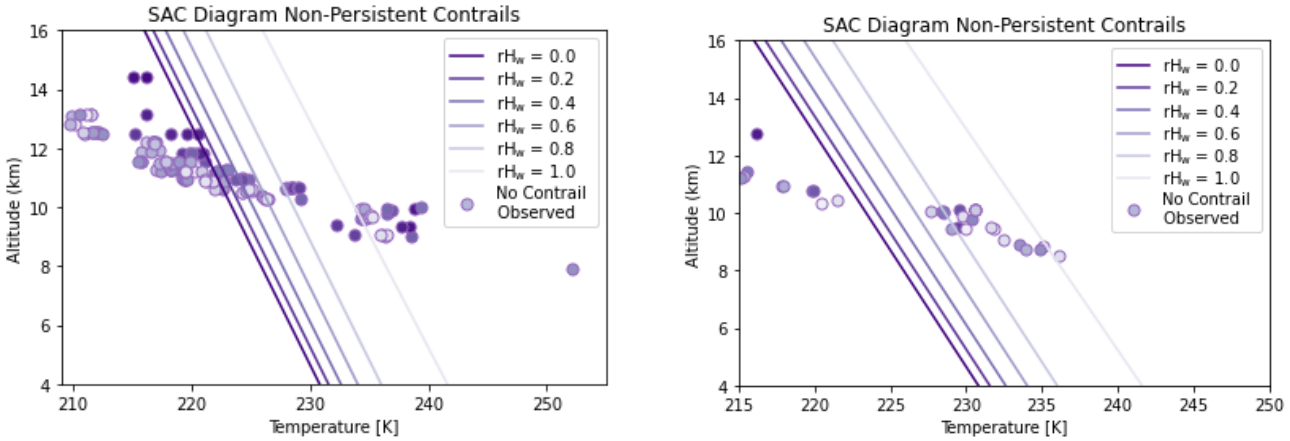

(a) SAC diagram for No or Non-Persistent Contrails, Florida (16 to 18 March 2020)

(b) SAC diagram for No or Non-Persistent Contrails, California (6, 8 to 10 May 2020)

Figure 7. **No contrail** or **non-persistent contrails** over Florida (a) and California (b). They either do not satisfy the Schmidt-Appleman criteria (SAC), or they are in an ice super saturated region (ISSR).

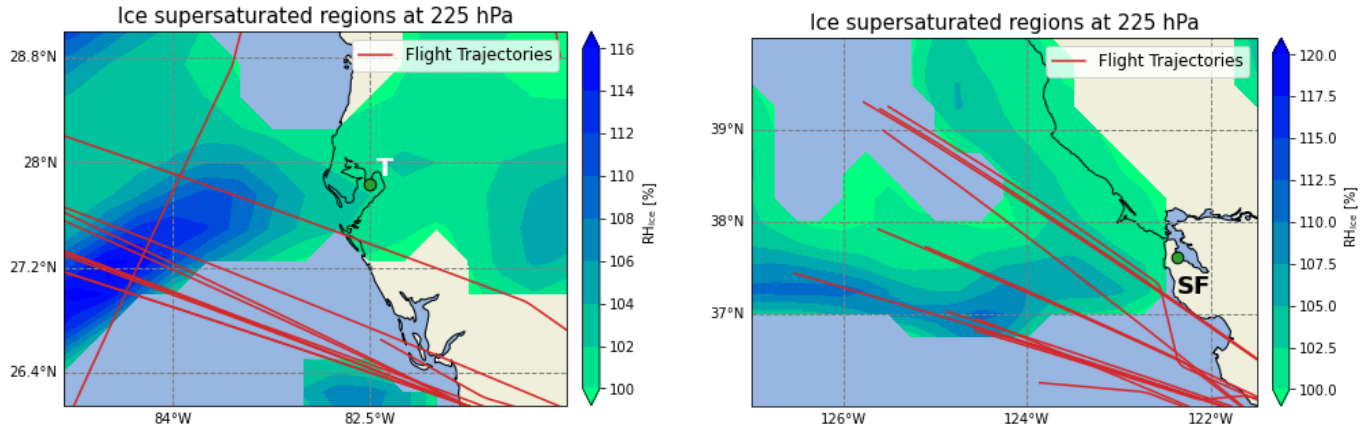

(a) ISSR for section of Florida, location of Tampa indicated by T (2020-03-18 18:00 UTC), with flight trajectories in red flying at cruise close to the ISSR.

(b) ISSR for section of California, location of San Francisco indicated by SF (2020-05-10 04:00 UTC), with flight trajectories in red flying at cruise close to the ISSR.

Figure 8. Two examples of ice-supersaturation regions in Florida and California. Clear area's indicate regions where $RH_{ice}<100\%$, that is the air is not supersaturated with respect to ice. The flight trajectories at cruise close to the ISSR are visualized by red lines. The limits of OpenSky's spatial coverage over oceans are also visible in Fig. 8b, with the trajectories stopping mid-flight over the ocean.

sesar JOINT UNDERTAKING 12th SESAR Innovation Days 5-8 December 2022, Budapest HungaroControl sesar DIGITAL ACADEMY

In Fig. 6, we see that *all* manual 'contrail' observations satisfy the SAC by either being in the 'Always Contrail' or 'Possible Contrail' parts of the graph. While not all 'contrail' observations are in an ISSR (27%), they will still be classified as 'persistent contrails', since in future climate-optimized routing model observations from remote sensing will take precedence over the ISSR criterion.

Eight cases of a 'no contrail' observation satisfy the SAC *and* the ISSR criterion. This means that in 8 cases (out of 235 flights), our manual detection does not agree with the theoretical persistent contrail formation. This indicates the uncertainty of the theoretical model when applying to real flight conditions.

In Fig. 7 the remaining 142 'no contrail' observations are plotted. Some of the plotted 'No contrail' observations do not satisfy SAC, and so no contrails form at all. While some observations do satisfy the SAC, they are *not* in an ISSR. Since both need to be satisfied to be predicted as a persistent contrail, all these 'no contrail' observations can be classified as 'non-persistent contrails'.

In Fig. 8, two examples are shown of ice-supersaturation regions in Florida and California, together with trajectories of flight flying at cruise near the altitude of the ISSR.

V. Discussion

In this paper, we manually labeled the contrails. However, an automatic contrail detection method, based on feature detection, image processing and machine learning methods is currently under development. As this is in the experimental phase, the results are not accurate enough to be included in this study. Clearly, manual observation and identification of contrail forming events is rather time consuming. While being impractical in this sense, the rigor of manual examination in accordance with the contrail forming models is beneficial. This is mainly because during aging of contrails, they diffuse and become increasingly difficult to distinguish from naturally formed cirrus clouds. Thus, in order to examine the contrail formation models accurately, correctly identifying contrails early on in the formation is essential.

In Fig. 6 the 'contrail' observations are all, without exception, categorized in the 'contrail' section of the SAC diagrams. This demonstrates that the open source data applied is of sufficient quality to predict whether contrails form based on atmospheric conditions. This is an essential part of the climate-optimal model under construction, since only then, can flight routes be partially optimized based on whether or not they create contrails.

While the majority (73%) of the 'contrail' observations in Fig. 6 are indeed in ISSR's, some (27%) are not, indicating that importance should be given to tracking contrail lifetime with GOES-16 imagery. In our climate optimized routing model, observations from the remote sensing data will be given priority over predictions from the SAC.

However, confirming where contrails *will not* form is more ambiguous. The 'no-contrail' observations are predicted with less accuracy. This accuracy greatly depends on the quantity of contrails that form throughout the day.

When discussing prediction accuracy it is often beneficial to refer to a confusion matrix, as seen in Table II. This is an effective way to summarize prediction results in a classification problem.

On days where an abundance of contrails occur, the True Negative prediction is higher (correctly predicting no contrails). On days with more intermittent contrail occurrence, or no contrails at all, there is a higher occurrence of False Positive events (incorrectly predicting no contrail observations as contrail forming events).

TABLE II. Observations and Prediction

		Actual Persistent Contrail	
		True	False
Predicted Persistent Contrails	Positive	True Positive	False Positive
	Negative	False Negative	True Negative

Summarizing Table III, we see that 204 (62+142) of our observations are correctly predicted (i.e. True Positive + True Negative) by the SAC and ISSR criterion. This is 87% of the total observations. Meanwhile, 31 (13%) do not agree with the theoretical models (i.e. False Positive + False Negative).

TABLE III. Results comparing Observations with Prediction

		Actual Persistent Contrail		
		True	False	Total
Predicted Per. Con.	Positive	62	8	70
	Negative	23	142	165
	Total	85	150	235

Nonetheless, the vast majority (95%) of no contrail' observations are classified correctly in the sections of 'possible' or 'never' contrails. This implies that for the eventual climate-optimal model an overestimation may occur of contrail formation. The model may find it necessary to reroute an aircraft because it predicts contrails will form, when in reality, no contrail formation would occur. Based upon this data set, unnecessary rerouting, and thus climate sub-optimization may occur in some 5% of the cases.

Even though not all 'no contrail' observations are categorized in the 'never contrails' section of the SAC diagram (Fig. 7), the model could still need to be applied to correctly classify them. The explanation for the classification of 'no Contrail' observations as 'possible contrail' or 'always contrail', is that there is an actual formation of contrails, however these are not persistent, this is confirmed by the lack of an ISSR. While the temporal resolution of GOES-16 at 5 minutes is quite high (by comparison in remote sensing), for detecting non-persistent contrails with lifetimes of just a few minutes it is insufficient. Non-persistent contrails have a small climate impact [13], and so for the purposes of the future climate-

optimal routing model, this 'insufficient' temporal resolution would be adequate.

In this case, flights should not be rerouted for a short lived warming contrail, which would have little climate impact. The results from this paper emphasise the importance of implementing the ISSR as well as the SAC distinction in the climate-optimization routing model. Additionally, these results show that the ISSR (persistence) condition is rarer, in the regions examined in this paper, than the theoretical formation condition, this implies that for the computational speed of our model, that ISSR conditions should be examined before the formation conditions. It should also be investigated whether the rarity of ISSR conditions still applies in other regions.

Literature [20]–[22] shows that it is more common to see contrail formation in conditions *warmer* than the Schmidt-Appleman Criterion. By contrast, in this research, all contrail observations occur in conditions *colder* than the SAC. In [20] the explanations given are; instrument and measurement uncertainties, or atmospheric variability and mixing in the exhaust. The latter leads to various non-equilibrium processes, that are not captured by the SAC.

Some of the observed contrails could potentially also be aerodynamic contrails, not exhaust contrails. These aerodynamic contrails are formed by the cooling effect of accelerated flow over aircraft wings [23]. A distinction between these can be made using the measured particle sizes, by sorting based on exceeding or falling below altitude-dependent particle size distributions [24]. Compared to exhaust contrails, aerodynamic contrails have a much smaller climate impact. However this may change with increasing air traffic in the tropics, since they are more likely to occur there, due to the high humidity [25]. Further research is required if their occurrence is frequent enough to be of relevance for the climate-optimized routing model and if so, how the formation of these aerodynamic contrails can be predicted.

The Schmidt-Appleman diagrams in the Results section clearly show a relation in altitude, with contrail-forming atmospheric conditions being present at higher altitudes (>11 km) or flight levels (>FL360). As described in the methodology a criteria was that flight should be at cruise, this makes it likely that most aircraft creating contrails in this analysis are long-haul flights, which fly at higher altitudes at cruise. Long-haul flights (>1000nm) have been shown to be more suitable for cost-effective climate-optimization, than short haul flights [26]. Usually an aircraft would climb (or, though less likely, descend) in order to avoid an ISSR, unless close to the edge of the region, where it might be more beneficial to fly around. This is already common practice with military aircraft, when they want to avoid detection, since creating contrails would make them easily discoverable. At higher altitudes the air density thins, and the air can hold less humidity, which makes presence of ISSR and contrail formation less likely. During a short flight, it is less likely for this changing of altitude to have a net positive climate impact.

Regarding the relative humidity of the ECMWF ERA-5 Reanalysis data, this model tends to underestimate the relative humidity close to saturation [27], [28]. This implies that the rH_w = 1.0 line, should be shifted to the left, to lower temperatures. For the majority of 'no contrail' observation points this has no impact on their classification, since their local relative humidity values are low enough not to end up on the 'contrail' section of the graph. This does mean however, that points with a higher relative humidity closer to the saturation line, may now be incorrectly classified as 'contrail' events, due to inaccuracies in the ERA-5 Reanalysis data, not due to the Schmidt-Appleman model.

Dates were selected to be within the early days of the COVID-19 pandemic, when the number of flights plummeted globally, because this served to benefit the attribution of individual flights to individual contrails. However, it should also be considered that the probability of contrail formation varies across months and seasons [8]. When creating the contrail detection model, dates outside the spring and summer seasons should also be considered to account for these differences.

VI. Conclusion & Future Work

Contrail formation models were examined using open flight and remote sensing data from multiple days with contrail formation. Manual categorization of an atmosphere as 'contrail forming' or 'not contrail forming' according to the Schmidt-Appleman Criterion and ISSR (ice-supersaturation region) condition, shows strong agreement between contrail observation and contrail prediction. Not only are persistent contrails predicted well, which is essential for our climate-optimal routing model, non-persistent contrails are also accurately predicted, which is of somewhat superfluous use for the model.

The results of this paper also show the importance of implementing the ISSR as well as the SAC distinction in the climate-optimization routing model. Since the ISSR (persistence) condition is less common than the formation condition, it would be beneficial to the computational speed of our model for that condition to be satisfied first.

However, in further research, an automated contrail detection model should be developed for determining the contrail persistence. The observations from remote sensing allow for contrail tracking throughout its lifetime, and will take precedence over the ice-supersaturation criterion.

Eventually, for climate-optimized routing model, characteristics, such as persistence, warming/cooling, energy forcing, related to contrail formation will need to be predicted based on atmospheric conditions. This examination contributes to the understanding of the atmospheric conditions under which contrails form, specifically regarding the threshold temperature and reinforce its dependence on altitude. This shows promise for the generation of a climate-optimal routing model based on open data using feature detection and machine learning.

References

[1] D. Lee, "The contribution of global aviation to anthropogenic climate forcing for 2000 to 2018." *Atmospheric Environment*, vol. 244, 2021.

[2] E. Roosenbrand, J. Sun, I. Dedoussi, D. Stam, and J. Hoekstra, "Assessing and modelling climate optimal flightsusing open surveillance and remote sensing data." *ICRAT 2022*.

[3] T. Roger, U. Schumann, and M. Stettler, "Beyond contrail avoidance: Efficacy of flight altitude changes to minimise contrail climate forcing." *Aerospace*, vol. 7, 2020.

[4] U. Burkhardt and B. Kärcher, "Global radiative forcing from contrail cirrus," *Nature Climate Change*, vol. 1, 2011.

[5] J. Molloy, R. Teoh, G. Harty, S.and Koudis, U. Schumann, I. Poll, and M. Stettler, "Design principles for a contrail-minimizing trial in the north atlantic." *Aerospace*, vol. 9, 2022.

[6] U. Schumann, K. Graf, and H. Mannstein, "Potential to reduce the climate impact of aviation by flight level changes." *3rd AIAA Atmospheric Space Environments Conference*, 2011.

[7] U. Schumann, "On conditions for contrial formation from aircraft exhausts." *Meteorol. Zeitschrift*, vol. 4-23, 1996.

[8] R. Dischl, S. Kaufmann, and C. Voigt, "Regional and seasonal dependence of the potential contrail cover and the potential contrail cirrus cover over europe." *Aerospace*, vol. 9, p. 485, 2022.

[9] J. Goff and S. Gratch, "Low-pressure properties of water from 160 to 212 f," *Transactions of the American Society of Heating and Ventilating Engineers, the 52nd Annual Meeting of the American Society of Heating and Ventilating.*, vol. 95-122, 1946.

[10] A. W. Service, "Forecasting aircraft condensation trails." *ADA111876*, 1981.

[11] U. Schumann, "Formation, properties and climatic effects of contrails." *Physique*, vol. 6:549–565, 2005.

[12] P. Ferris, "The formation and forecasting of condensation trails behind modern aircraft." *Meteorological Applications*, vol. 3, 2007.

[13] B. Kärcher, "Formation and radiative forcing of contrail cirrus." *Nat. Commun.*, vol. 9, 2018.

[14] M. Schrader, "Calculations of aircraft contrail formation critical temperatures." *Journal of Applied Meteorology*, vol. 36-12, p. 1725–1729, 1997.

[15] M. Vázquex-Navarro, H. Mannstein, and S. Kox, "Contrail life cycle and properties from one year of MSG/SEVIRI rapid-scan images." *Atmos. Chem. Phys.*, vol. 15, 2015.

[16] D. Avila, L. Sherry, and T. Thompson, "Reducing global warming by airline contrail avoidance: A case study of annual benefits for the contiguous united states." *Transportation Research Interdisciplinary Perspectives*, vol. 2, 2019.

[17] X. Sun, S. Wandelt, C. Zheng, and A. Zhang, "Covid-19 pandemic and air transportation: Successfully navigating the paper hurricanes," *Journal of Air Transport Management.*, vol. 94, 2021.

[18] M. Strohmeier, O. Xavier, L. Jannis, M. Schäfer, and V. Lenders, "Crowdsourced air traffic data from the opensky network 2019–2020." *Journal of Air Transport Management*, vol. 94, 2021.

[19] D. Dee, S. Uppala, A. J. Simmons, P. Berrisford, P. Poli, and S. Kobayashi, "The era-interim reanalysis: configuration and performance of the data assimilation system." *Quarterly Journal of the Royal Meteorological Society*, vol. 137, 2011.

[20] T. Bräuer, C. Voigt, S. Sauer, D.and Kaufmann, V. Hahn, and M. Scheibe, "Airborne measurements of contrail ice properties— dependence on temperature and humidity." *Geophysical Research Letters*, vol. 48, 2021.

[21] J.-F. Gayet, G. Febvre, G.and Brogniez, W. Chepfer, H.and Renger, and P. Wendling, "Microphysical and optical properties of cirrus and contrails: Cloud field study on 13 october 1989." *Journal of the Atmospheric Sciences*, vol. 53, 1996.

[22] E. J. Jensen, O. B. Toon, S. Kinne, G. W. Sachse, B. E. Anderson, and K. R. Chan, "Environmental conditions required for contrail formation and persistence." *Journal of Geophysical Research*, vol. 103, 1998.

[23] K. Gierens, B. Kärcher, and B. Mannstein, H.and Mayer, "Aerodynamic contrails: Phenomenology and flow physics." *Journal of the At- mospheric Sciences*, vol. 66, 2009.

[24] K. Gierens, M. K. Ästner, and D. K. Klatt, "Iridescent aerodynamic contrails: The norderney case of 27 june 2008." *Meteorologische Zeitschrift*, vol. 20, 2011.

[25] K. Gierens and F. Dilger, "A climatology of formation conditions for aerodynamic contrails." *Atmos. Chem. Phys.*, vol. 13, 2013.

[26] N. Chen, P. Kirschen, B. Sridhar, and H. Ng, "Identification of flights for cost-efficient climate impact reduction," *AIAA AVIATION 2014 - AIAA/3AF Aircraft Noise and Emissions Reduction Symposium.*, 2014.

[27] A. Kunz, N. Spelten, P. Konopka, R. Müller, R. Forbes, and H. Wernli, "Comparison of fast in situ stratospheric hygrometer (fish) measurements of water vapor in the upper troposphere and lower stratosphere (utls) with ecmwf (re)analysis data." *Atmos. Chem. Phys*, vol. 14, 2014.

[28] M. Weger, B. Heinold, U. Engler, C.and Schumann, R. Seifert, A.and Fößig, and H. B. U. B. S. Voigt, C.and Baars, "The impact of mineral dust on cloud formation during the saharan dust event in april 2014 over europe." *Atmos. Chem. Phys.*, vol. 18, 2018.